













Scar conducting channel characterization to predict arrhythmogenicity during ventricular tachycardia ablation

Paula Sanchez-Somonte^{1,2,3}, Paz Garre ^{1,2}, Sara Vázquez-Calvo^{1,2},
Levio Quinto^{1,2}, Roger Borràs ^{1,2}, Susanna Prat^{1,2}, Jose T. Ortiz-Perez ^{1,2},
Martin Steghöfer ⁴, Rosa M. Figueras i Ventura ⁴, Eduard Guasch ^{1,2,3},
José Maria Tolosana ^{1,2,3}, Elena Arbelo ^{1,2,3}, Josep Brugada ^{1,2}, Marta Sitges ^{1,2,3},
Lluís Mont ^{1,2,3}, and Ivo Roca-Luque ^{1,2,3*}

¹Cardiology Department, Institut Clinic Cardiovascular, Universitat de Barcelona, Hospital Clinic, Villarroel 170, 08036, Barcelona, Spain; ²Cardiology Department, Institut d'Investigacions Biomèdiques August Pi i Sunyer (IDIBAPS), Hospital Clinic, Villarroel 170, 08036, Barcelona, Spain; ³Centro de Investigación Biomédica en Red de Enfermedades Cardiovasculares (CIBERCV), Av.Monforte de Lemos, 3-5. Pabellon 11. Planta 0. 29029, Madrid, Spain; and ⁴Adas3D Medical S.L, C/Paris 179, 08036, Barcelona, Spain

Received 29 June 2022; accepted after revision 1 November 2022; online publish-ahead-of-print 4 January 2023

Aims

Heterogeneous tissue channels (HTCs) detected by late gadolinium enhancement cardiac magnetic resonance (LGE-CMR) are related to ventricular arrhythmias, but there are few published data about their arrhythmogenic characteristics.

Methods and results

We enrolled 34 consecutive patients with ischaemic and non-ischaemic cardiomyopathy who were referred for ventricular tachycardia (VT) ablation. LGE-CMR was performed prior to ablation, and the HTCs were analyzed. Arrhythmogenic HTCs linked to induced VT were identified during the VT ablation procedure. The characteristics of arrhythmogenic HTCs were compared with those of non-arrhythmogenic HTCs. Three patients were excluded due to low-quality LGE-CMR images. A total of 87 HTCs were identified on LGE-CMR in 31 patients (age: 63.8 ± 12.3 years; 96.8% male; left ventricular ejection fraction: $36.1 \pm 10.7\%$). Of the 87 HTCs, only 31 were considered arrhythmogenic because of their relation to a VT isthmus. The HTCs related to a VT isthmus were longer [64.6 ± 49.4 vs. 32.9 ± 26.6 mm; OR: 1.02; 95% CI: (1.01–1.04); $P < 0.001$] and had greater mass [2.5 ± 2.2 vs. 1.2 ± 1.2 grams; OR: 1.62; 95% CI: (1.18–2.21); $P < 0.001$], a higher degree of protectedness [26.19 ± 19.2 vs. 10.74 ± 8.4 ; OR 1.09; 95% CI: (1.04–1.14); $P < 0.001$], higher transmural thickness [number of wall layers with CCs: 3.8 ± 2.4 vs. 2.4 ± 2.0 ; OR: 1.31; 95% CI: (1.07–1.60); $P = 0.008$] and more ramifications [3.8 ± 2.0 vs. 2.7 ± 1.1 ; OR: 1.59; 95% CI: (1.15–2.19); $P = 0.002$] than non-arrhythmogenic HTCs. Multivariate logistic regression analysis revealed that protectedness was the strongest predictor of arrhythmogenicity.

Conclusion

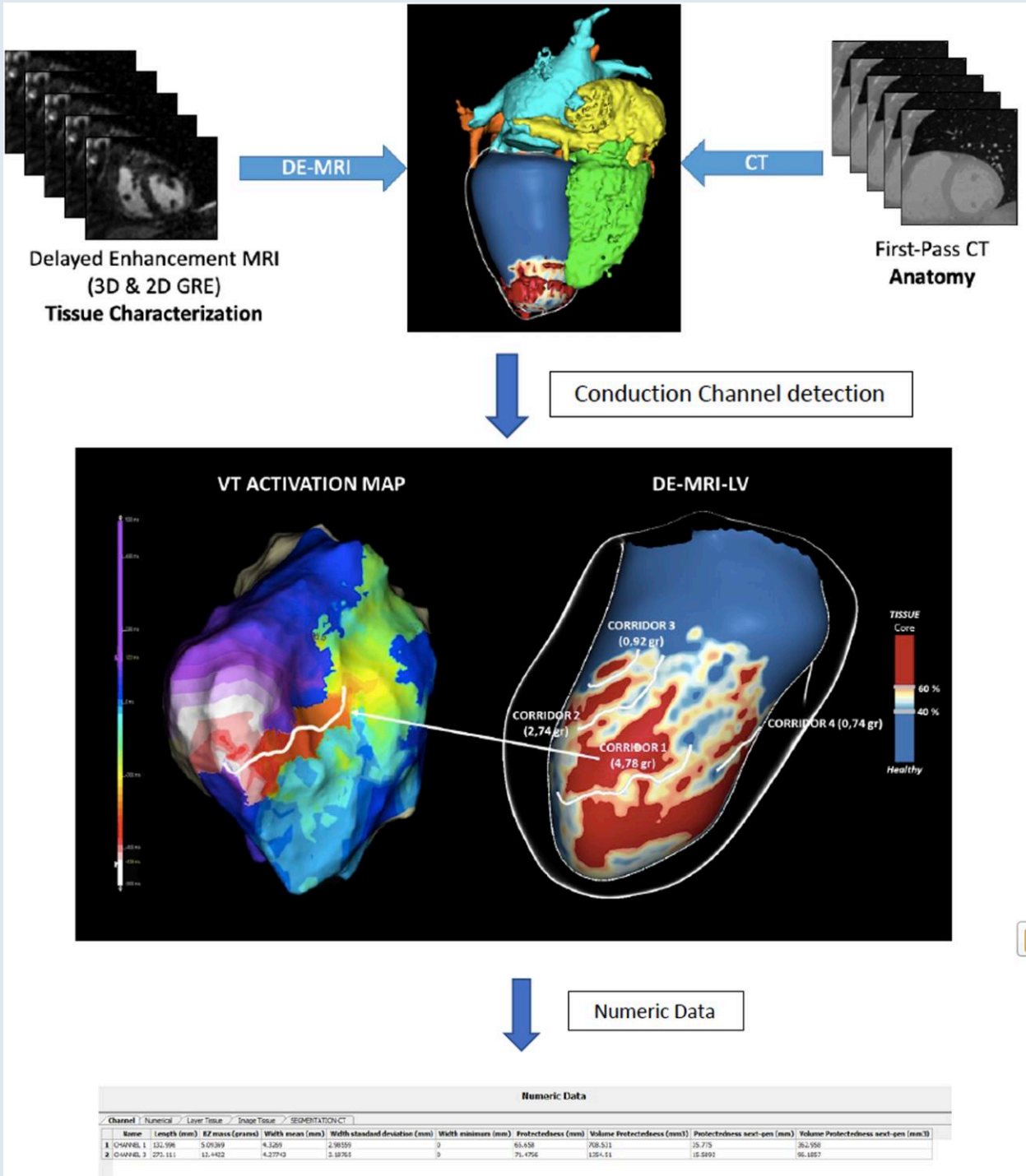
The protectedness of an HTC identified by LGE-CMR is strongly related to its arrhythmogenicity during VT ablation.

* Corresponding author. Tel: 00 34 617 48 17 36, E-mail address: iroca@clinic.cat

© The Author(s) 2023. Published by Oxford University Press on behalf of the European Society of Cardiology.

This is an Open Access article distributed under the terms of the Creative Commons Attribution-NonCommercial License (<https://creativecommons.org/licenses/by-nc/4.0/>), which permits non-commercial re-use, distribution, and reproduction in any medium, provided the original work is properly cited. For commercial re-use, please contact journals.permissions@oup.com

Graphical Abstract



Keywords

Ventricular tachycardia • cardiac magnetic resonance • scar • heterogeneous tissue channel • conducting channel

What's new?

- Scar channel characteristics (length, mass, transmural, protectedness...) can be measured by LGE-CMR.
- Scar channel characteristics are related to arrhythmogenicity during a ventricular tachycardia ablation procedure.
- The protectedness, which is the measure of the length of the protected part (the isthmus) of a given conducting channel, is strongly related to arrhythmogenicity.

Introduction

Scar-related re-entry is the most common arrhythmia substrate in patients with episodes of monomorphic ventricular tachycardia (VT).¹ This re-entry is caused by the presence of slow conduction areas within the scar that connect to the healthy non-scarred myocardium. These regions, also called slow conducting channels (CCs), can be accurately identified from the electroanatomical maps (EAMs) obtained during VT ablation procedures.^{2,3}

Likewise, this heterogeneous tissue that acts as a VT isthmus can also be easily identified as heterogeneous tissue channels (HTCs) on late gadolinium enhancement cardiac magnetic resonance (LGE-CMR) and correlates well with the CCs identified in the EAMs.⁴

In recent years, efforts have focused on better definition of the arrhythmogenic substrate, and CCs have been a target for substrate ablation of VT in order to improve the results.⁵ Given the good correlation between the HTCs observed on LGE-CMR and the CCs observed on EAMs,⁴ LGE-CMR has been attracting growing interest for use in the identification of arrhythmic substrates.⁶⁻⁸

The relation between HTCs and arrhythmogenicity has been demonstrated before in patients with implantable cardioverter-defibrillators (ICDs) implanted for primary prevention in whom the presence of HTCs on the LGE-CMR was related to the presence of ICD therapies during the follow-up.⁹

On the other hand, the challenge of obtaining high-quality images in patients with ICDs, which cause imaging artefacts, has been solved by the introduction of a new wideband (WB) sequence that allows the elimination of these artefacts.¹⁰

However, even though several groups have previously reported the use of LGE-CMR to guide VT ablation procedures, we are not aware of any published data on the specific HTC characteristics related to arrhythmogenicity.

The aim of this study was to analyze the usefulness of imaging for evaluating the characteristics of HTCs and relate them to arrhythmogenicity during a VT ablation procedure.

Methods

Patients

We enrolled 34 consecutive patients with ischaemic and non-ischaemic cardiomyopathy with an ICD implanted for primary or secondary prevention who were referred for a VT ablation procedure. The study was approved by the institutional ethics committee.

LGE-CMR acquisition and processing

All cardiac LGE-CMR studies were performed with a 1.5 T MAGNETOM Trio scanner (Siemens Healthcare, Erlangen, Germany) using a WB sequence to prevent artefacts.

LGE-CMR images were processed with ADAS 3D software (ADAS 3D, ADAS3D Medical S.L.) following a previously described protocol.^{5,9,10} In brief, left ventricular (LV) endocardial and epicardial borders were automatically delineated (and manually corrected if necessary) using three anatomical landmarks (LV apex, mitral, and aortic rings). Nine concentric surface layers were created automatically from the endocardium to the epicardium at

10–90% of the LV wall thickness. A 3D shell was created for each layer. Scar areas were characterized as core and border zone (BZ) using an algorithm based on maximum pixel signal intensity (SI) in the LV wall. The automatic algorithm classified pixels with SI >60% of the maximum pixel as core, SI between 40% and 60% as BZ and SI <40% as healthy tissue. This threshold-based classification was visualized in 3D through colour-coded SI maps (Figure 1).

Identification and characterization of HTCs on LGE-CMR

The HTC identification was performed automatically by the software. HTC candidates were defined as paths of BZ tissue (with the prespecified pixel SI threshold) starting and ending in healthy tissue and protected by core areas on both sides or by a core area on one side and a valve annulus on the other (Figure 1). Each layer was divided by the software in the 17-segment model described by the American Heart Association (AHA).

In the case that a HTC was identified in adjacent layers at the same AHA segment with the same orientation, it was considered as a single channel. The software also analyzed automatically the length, width and mass of each HTC. The number of ramifications was considered the sum of the total numbers of entrances and exits seen in the LGE-CMR of each HTC (Figure 1).

Protectedness

Protectedness is a measure of the length of the protected part (the isthmus) of an HTC. It is automatically calculated by the software. To calculate it, the degree of protection by core tissue of every point of a given HTC centerline was analyzed. To do so, at each point of an HTC centerline, the percentage of the perimeter of a HTC with core tissue, healthy tissue or only BZ tissue inside a 3.5 mm distance was analyzed. If both core and healthy tissue were present along a given direction, only the tissue type closest to the HTC centerline was considered. Based on these percentages, the local protectedness of the point was determined: If healthy was found anywhere, the local protectedness was set to zero. If no healthy tissue was found, then the percentage of the perimeter that coincided with core tissue determined the local protectedness. Having less than 15% core yielded a local protectedness of 0% (fully unprotected HTC point), and having more than 40% yielded a local protectedness of 100% (fully protected HTC point). Core values between 15% and 40% (partially protected HTC points) were mapped linearly to local protectedness values between 0% and 100%. Finally, the local protectedness values were integrated over the centerline of the whole HTC. To illustrate the meaning of the final protectedness value, we present two examples. A HTC measuring 5 mm with 100% protectedness everywhere would have a protectedness value of 5 mm. However, a HTC corridor measuring 10 mm with 50% protectedness everywhere would also have a protectedness of 5 mm (Figure 2).

All parameters of the protectedness formula (3.5 mm ray length, lower and upper cut-off values of 15% and 40% respectively for the core surrounding percentage limits) were determined using a parameter fitting against a binary ground truth defined by a clinical expert. At first, the HTCs were detected in multiple cases. Then the expert decided for all detected HTCs, which ones could be slow conduction channels and which ones were too superficial. Finally, the local protectedness values were integrated over the whole unified centerline. The integration includes possible bifurcations, effectively leading to a protectedness value that is the sum of the protectedness values integrated over each branch.

VT ablation protocol and CC identification on the EAM

Procedures were performed under general anaesthesia. Access to the left ventricle was achieved with a transeptal and/or retrograde aortic approach. Epicardial mapping was performed in cases when an epicardial origin of VT was suspected.

A substrate voltage map of the LV was obtained during right ventricular paced rhythm for better stability of the cardiac cycle using an HD Grid catheter and Ensate Precision (Abbott Medical, USA).

Peak-to-peak amplitudes of 0.5 to 1.5 mV and <0.5 mV were initially used to define the low-voltage zone and the dense scar zone, respectively. Activation mapping was analyzed simultaneously by using the Last Deflection algorithm™ in the navigation system (Abbot Medical, USA). LAVAs and late potentials (LPs) were manually tagged.

After activation, voltage mapping and tagging of LAVAs and LPs, analysis of deceleration zones (DZs) was performed. After delineation of slow

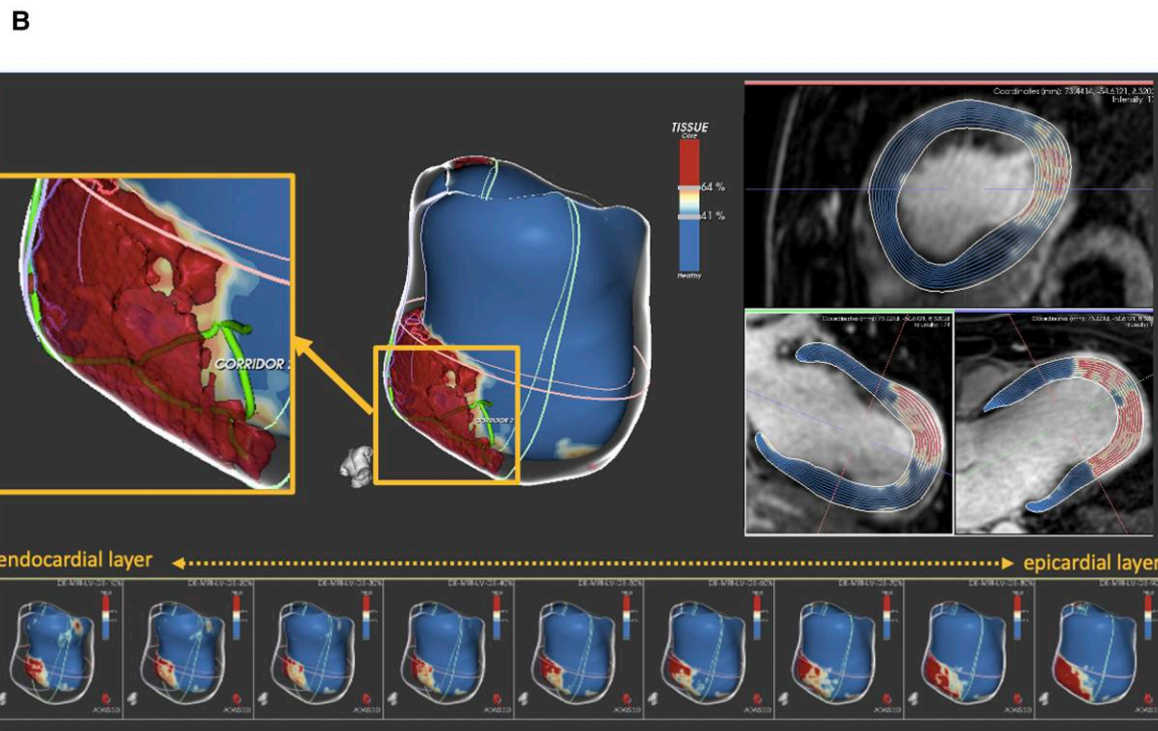
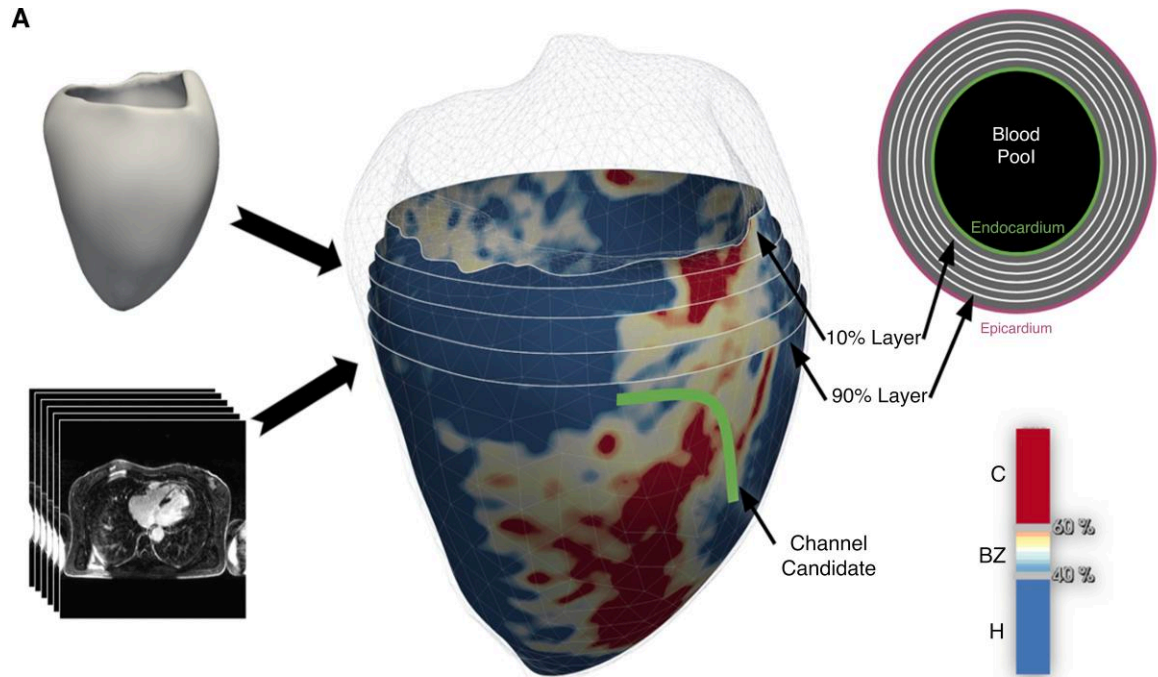


Figure 1 LGE-CMR reconstruction of the LV with an anterolateral scar in the superior panel (A) and an anteroapical scar in the inferior panel (B). We can distinguish the core and BZ from the healthy myocardium. A line is drawn over the surface representing a conducting channel (A,B). We can see substrate evolution through different layers, from the endocardium (10–30%) to the epicardium (70–90%). LGE-CMR = late gadolinium enhancement cardiac magnetic resonance; LV = left ventricle; BZ = border zone.

conduction areas, the HD grid catheter was positioned in a potential area of the VT isthmus (slow conduction area and/or channel isthmus according to LGE-CMR images), and the VT induction protocol was performed. When

VT was haemodynamically tolerated, activation mapping was performed. In cases in which VT was not haemodynamically tolerated, the VT isthmus was defined as the area with a fast transition of good pace mapping and

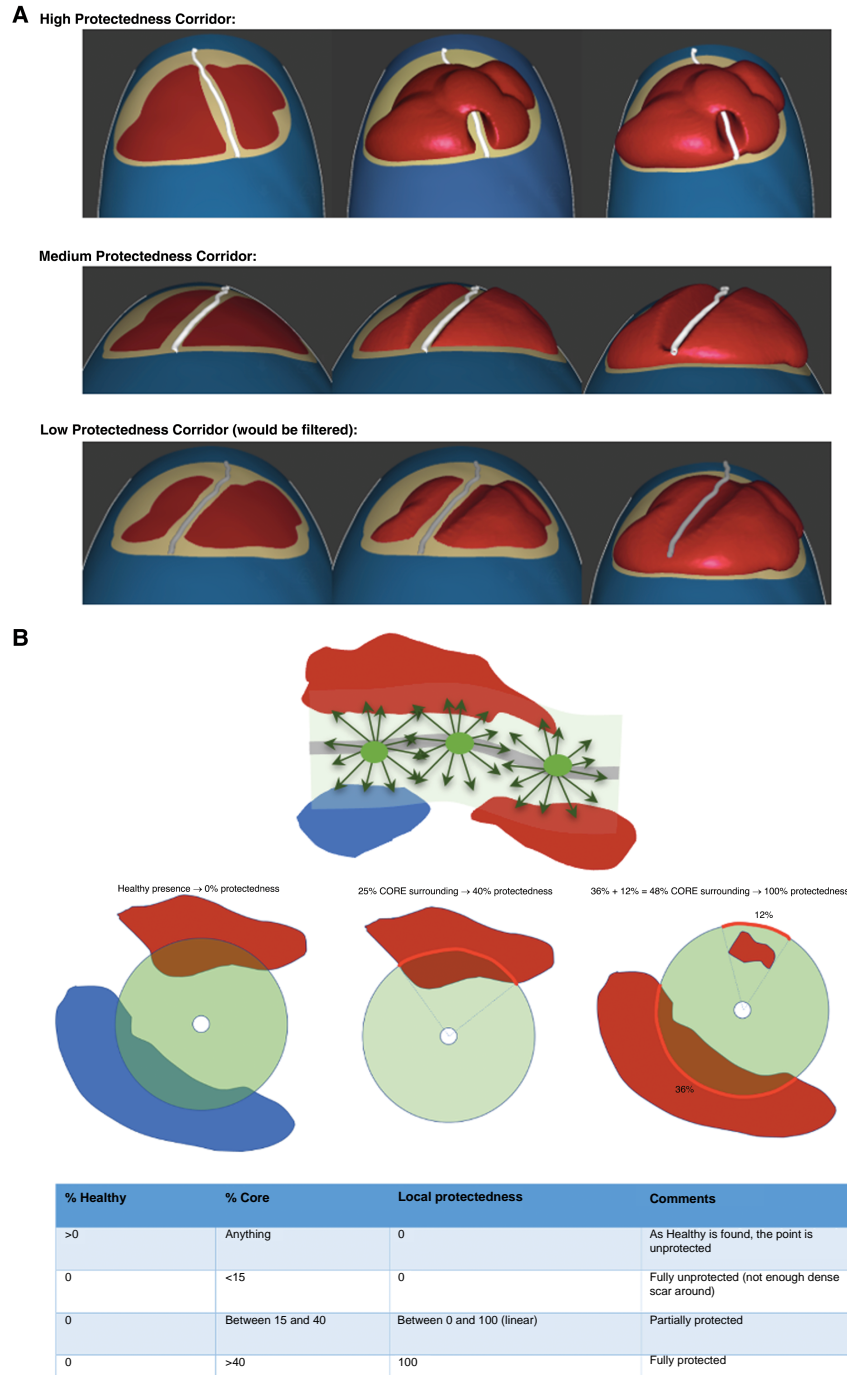


Figure 2 Protectedness Panel (A) Protectedness: measure of the length of the protected part (the isthmus) of a corridor. Three examples of HTC with high protectedness, medium protectedness and low protectedness, respectively. HTC = heterogeneous tissue channel Panel (B) Protectedness computation: HTC centerline surrounded by the area of analysis for protectedness and nearby core and/or healthy tissue The percentages of HTCs that had core tissue, healthy tissue or only border-zone tissue were analyzed within a 3.5 mm distance. Based on these percentages, the local protectedness of the point was determined: If healthy tissue was found anywhere, the local protectedness was set to zero. If no healthy tissue was found, then the percentage of the perimeter that coincided with core tissue determined the local protectedness. Having less than 15% core yielded a local protectedness of 0%, and having more than 40% yielded a local protectedness of 100% (fully protected corridor point). Core values between 15% and 40% (partially protected corridor points) were mapped linearly to local protectedness values between 0% and 100%. Finally, the local protectedness values were integrated over the whole centerline of the corridor, yielding the length of the protected part of the corridor. HTC = heterogeneous tissue channel.

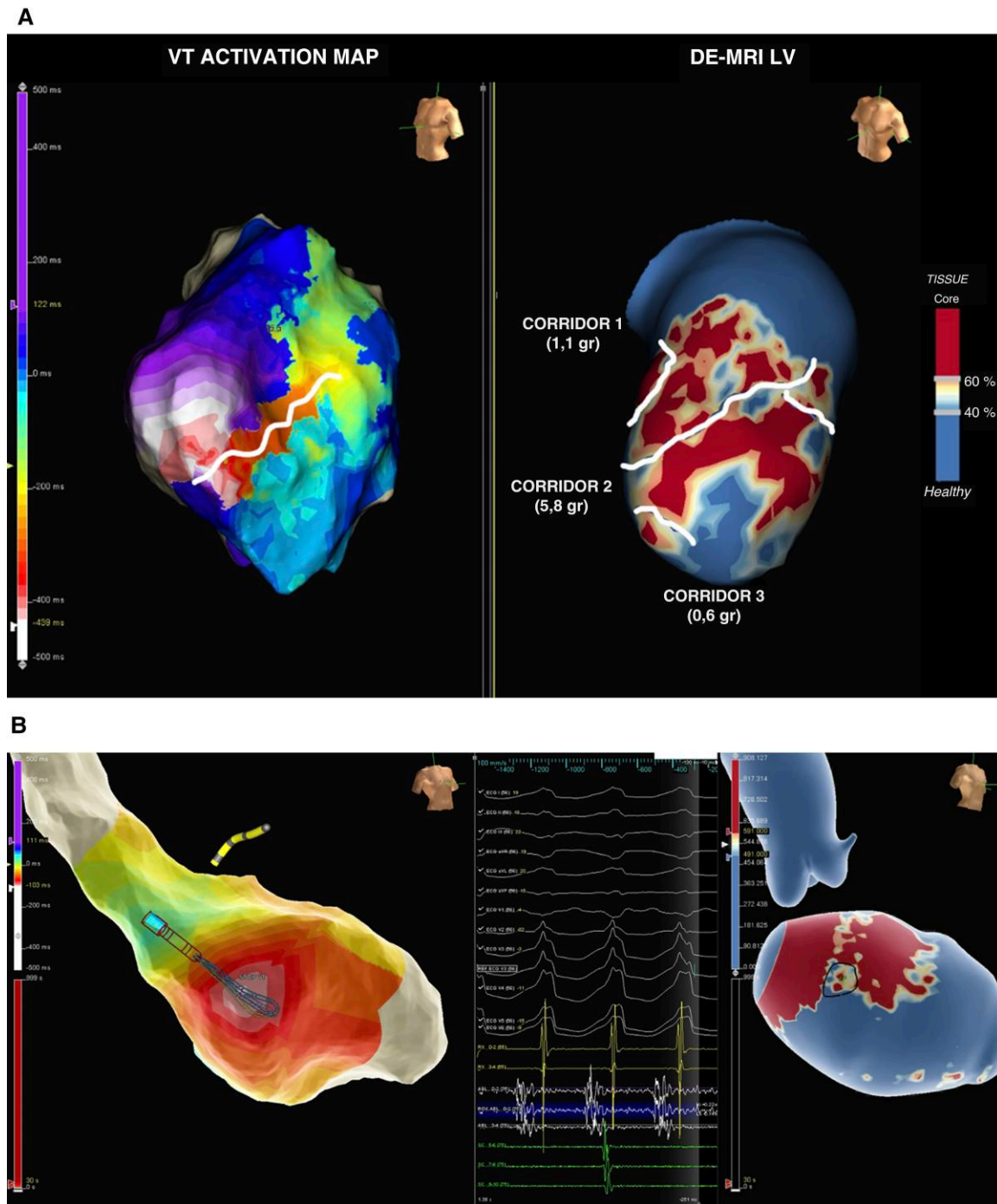


Figure 3 Comparison between the EAM from the VT procedure and LGE-CMR. Panel (A) Left: Activation mapping during VT. Right: LGE-CMR reconstruction of the LV (core, BZ and healthy myocardium are represented). The entire VT cycle length and the diastolic path are located in the anterolateral region of the LV. CMR shows an anterolateral scar and three HTC (lines). The CC used by the VT on the EAM corresponds to HTC number 2 on CMR, which has a greater BZ mass than the others (5.8 g vs. 1.1 corridor 1 and 0.6 g corridor 3). Panel (B) An example of mid-myocardial VT is shown. EAM shows a focal activation pattern with the earliest activation site in the midseptum, with presystolic electrograms. LGE-CMR shows an intramural septal scar (40% layer is shown) with an HTC (line) in the same spot of the earliest activation site. EAM = electroanatomic map. VT = ventricular tachycardia. LGE-CMR = late gadolinium enhancement cardiac magnetic resonance. LV = left ventricle. BZ = border zone. CC = conducting channel. CMR = cardiac magnetic resonance. HTC: heterogenous tissue channel.)

Table 1 Baseline patient and procedure characteristics

Baseline characteristics	Total population (n = 31)
Age (years)	63.8 ± 12.3
Male sex	96.8%
Ischaemic cardiomyopathy	74.2%
Smoker	16.1%
Hypertension	64.5%
Diabetes	54.8%
Dyslipidaemia	64.5%
LVEF	36.1 ± 10.7
Beta-blocker therapy	54.8%
Sotalol therapy	12.9%
Amiodarone therapy	64.5%
Antiarrhythmic drugs Class I	3.2%
Procedural characteristics	
Transeptal access	27 (87.1%)
Arterial access	17 (54.8%)
Epicardial access	2 (6.5%)
Procedural time (minutes)	229.8 ± 42.7
RX doses (mGy)	274.7 ± 172.6

LVEF, left ventricular ejection fraction; mGy, Milligray.

poor pace mapping. Radiofrequency (RF) was delivered using an externally irrigated 3.5 mm tip ablation catheter with 45°C temperature control, a 40–50 W power limit, and a 26–30 mL/min irrigation rate. In cases in which induced VT permitted activation mapping, the primary target for ablation was the central isthmus during re-entrant VT. In cases in which pace mapping was used to determine the VT isthmus, the first ablation target was the defined isthmus. After VT isthmuses were targeted, substrate ablation was performed. The main targets were the DZs and the entrances and exits of defined CCs. Remapping with an HD grid catheter was performed to detect residual substrate. Additional RF lesions were delivered if needed.

Definition of arrhythmogenicity of HTC on LGE-CMR

The LGE-CMR shells were integrated into the navigation system, and PSI maps were visualized side by side and compared with the EAM. The location (AHA segment) and orientation of the HTC identified in the CMR were compared with the VT isthmus annotated in the EAM (Figure 3). A given HTC was considered arrhythmogenic if it was located in the same AHA segment with the same orientation as the VT isthmus in the EAM identified by activation, entrainment mapping or pacemapping.

Statistical analysis

Continuous variables were compared with Student's *t* test. Categorical variables were compared using the chi-square test. Logistic regression analysis was used to study the effects of LGE-CMR characterization to predict arrhythmogenicity. Statistical analysis was performed using R software for Windows version 4.0.5 (R project for Statistical Computing; Vienna, Austria).

Results

Clinical data and procedure characteristics

A total of 34 patients who underwent WB CMR prior to a VT ablation procedure were included. Three patients were excluded because of low-quality LGE-CMR images. Finally, 31 patients were evaluated.

Table 2 Baseline channel characteristics

Channel characteristics	Total number of channels = 87
Number of channels per patient	2.8
Length (mm)	44.2 ± 39.2
Mass (grams)	1.6 ± 1.8
Width (mm)	4.9 ± 2
Protectedness	16.2 ± 15.1
Number of layers	2.9 ± 2.3
Number of ramifications	3.1 ± 1.6
Number of AHA segments	2.2 ± 1.0
Conducting channel location:	
Anterior	21 (24.1%)
Inferior	30 (34.5%)
Lateral	4 (4.6%)
Septal	14 (16.1%)
Apical	18 (20.7%)
Conducting channel layer location:	
Endocardium	44 (50.6%)
Mesocardium	13 (14.9%)
Epicardium	14 (16.1%)
Transmural	16 (18.4%)

Mm, millimetre; AHA, American Heart Association.

Transseptal approach was performed in 27 patients (87.1%) and retroaortic approach in 17 patients (54.8%). Epicardial access was used in 2 patients. A total of 31 VTs were induced (1 VT per patient). After the first inducible VT, an extensive substrate ablation was performed in all cases. Following substrate ablation, all patients remained non-inducible. Mean procedure time was 229.8 ± 42.7 min. Thirty-one VT isthmus were identified. In 25 patients (80.64%), the isthmus was determined by activation mapping and in six patients (19.35%) by pacemapping. (Baseline patient and procedure characteristics are listed in Table 1).

Channel identification and comparison between the EAM and CMR

From 31 patients, a total of 87 HTCs were identified on the LGE-CMR images. The average number of HTCs per patient on LGE-CMR was 2.8. The average number of layers affected by each channel was 2.9 ± 2.3, and the average number of AHA segments affected was 2.2 ± 1.0. Fifty percent of the HTCs were purely endocardial. Of the 87 HTCs identified on LGE-CMR, only 31 were considered arrhythmogenic because of their relation to the VT isthmus. The rest of the channels (56) were not related to induced VT in the ablation procedure. (HTCs characteristics are shown in Table 2).

Predictors of arrhythmogenicity

Regarding the baseline HTC parameters, the univariate analysis (Table 3) revealed that HTCs related to a VT isthmus were longer [64.6 ± 49.4 vs. 32.9 ± 26.6; OR: 1.02, 95% CI: (1.01–1.04); *P* < 0.001], had a higher mass [2.5 ± 2.2 vs. 1.2 ± 1.2; OR: 1.62, 95% CI: (1.18–2.21); *P* < 0.001] and had a higher degree of protectedness [26.19 ± 19.2 vs. 10.74 ± 8.4; OR: 1.09, 95% CI: (1.04–1.14); *P* < 0.001] than those that were not related to a VT isthmus. HTC width was not significantly associated with arrhythmogenicity.

Table 3 Univariate analysis of channel characteristics and the primary endpoint (arrhythmogenic channels)

All n = 87	Not arrhythmogenic (n = 56)	Arrhythmogenic (n = 31)	OR	95% CI	P
Length (mm)	32.9 ± 26.6	64.6 ± 49.4	1.02	(1.01–1.04)	<0.001
Mass (grams)	1.2 ± 1.2	2.5 ± 2.2	1.62	(1.18–2.21)	<0.001
Width (mm)	4.9 ± 2	4.9 ± 2.1	1.00	(0.80–1.25)	0.975
Protectedness	10.7 ± 8.4	26.2 ± 19.1	1.09	(1.04–1.14)	<0.001
Transmurality (number of layers affected by the CC)	2.4 ± 2.0	3.8 ± 2.4	1.31	(1.07–1.60)	0.008
Number of ramifications	2.7 ± 1.1	3.8 ± 2.0	1.59	(1.15–2.19)	0.002
Number of AHA segments	1.9 ± 0.8	2.7 ± 1.2	2.37	(1.4–4.04)	<0.001
Layers:					
Endocardium	26 (46.4%)	18 (58.1%)	1 (Ref)		
Mesocardium	12 (21.4%)	1 (3.2%)	0.12	(0.01–1.01)	0.051
Epicardium	9 (16.1%)	5 (16.1%)	0.8	(0.22–2.79)	0.73
Transmural	9 (16.1%)	7 (22.6%)	1.12	(0.35–57)	0.844
Location:					
Inferior	20 (35.7%)	10 (32.3%)	1 (Ref)		
Anterior	11 (19.6%)	10 (32.3%)	1.82	(0.58–5.71)	0.306
Lateral	2 (3.6%)	2 (6.5%)	2	(0.24–16.36)	0.518
Apical	15 (26.8%)	3 (9.7%)	0.4	(0.09–1.71)	0.217
Septal	8 (14.3%)	6 (19.4%)	1.5	(0.41–1.71)	0.542

OR, odds ratio; Ref, reference; CI, confidence interval; mm, millimetres; CC, conducting channel; AHA, American Heart Association. Bold values mean that there the values are statistically significant.

According to the layer location, no differences were found regarding whether the HTC were located in the endocardium, mesocardium or epicardium, but arrhythmogenic HTCs affected more layers (higher transmural) than non-arrhythmogenic HTCs [3.8 ± 2.4 vs. 2.4 ± 2.0, OR: 1.31, 95% CI: (1.07–1.60); *P* = 0.008]. In the same sense, arrhythmogenic HTCs affected more AHA segments than non-arrhythmogenic HTCs [2.7 ± 1.2 vs. 1.9 ± 0.8, OR: 2.37, 95% CI: (1.4–4.04); *P* < 0.001]. The location of the HTCs was not related to arrhythmogenicity.

Finally, the number of HTC ramifications (the total number of entrances and exits of each HTC) was also related to arrhythmogenicity [3.8 ± 2.0 vs. 2.7 ± 1.1, OR: 1.59, 95% CI: (1.15–2.19); *P* = 0.002]. Figure 4 shows the relation between the LGE-CMR HTC parameters and arrhythmogenicity.

When multivariable logistic regression analysis was performed (Table 4) with the covariables length, mass, number of layers affected (transmurality), number of ramifications, number of AHA segments affected and protectedness, only protectedness was still a predictor of arrhythmogenicity (Table 4). There was no difference in protectedness between ischaemic and non-ischaemic cardiomyopathy (15.61 ± 15.41 vs. 18.49 ± 14.17; *P* = 0.47).

A ROC curve was computed for protectedness, and the best cut-off point [AUC: 0.77 (0.66–0.88)] was 13.0 with a sensitivity of 74.2%, specificity of 69.6%, positive predictive value of 57.5 and negative predictive value of 83%. At this cut-off point of protectedness (>13), OR was 6.6, 95% CI: (2.46–17.67); *P* < 0.001.

Discussion

Over the last few years, the importance of cardiac imaging for patients with VT has increased exponentially because of its ability to define VT substrate with a high degree of detail.¹¹ The relationship between the CCs on the EAM and the HTCs on CMR has already been demonstrated,^{4,7,10} but this is the first study to analyze which characteristics of HTCs are related to arrhythmogenicity.

Our study suggests that arrhythmogenicity differs depending on channel characteristics such as length, transmural, ramifications and, in particular, protectedness. The present study is the first to show that LGE-CMR and its postprocessing with specific software

are useful not only for identifying HTCs but also for defining the arrhythmogenicity of each channel.

The presence of CCs has been related before to ventricular arrhythmias (VAs),⁹ but why patients with the same number of HTCs have a very different burden of VAs and why some HTCs, but not others, are related to the VT isthmus are not clear. To address this question, this work meticulously analyses several HTC characteristics, such as the length, transmural, protectedness and ramifications of each HTC on LGE-CMR and its relation to CC arrhythmogenicity.

Predictors of arrhythmogenicity

In our cohort of 31 patients, we found an average of 2.8 HTCs per person, and we observed that the arrhythmogenic HTCs were those with higher mass and length. We also found that those HTCs that occupied more AHA segments were more arrhythmogenic, which seems logical if the length is a predictor of arrhythmogenicity. Similarly, transmural and ramifications were important predictors of arrhythmogenicity. In terms of location, we did not find differences in whether HTCs were located predominantly in the anterior, posterior, septal, apical or lateral wall.

However, the most interesting characteristic of the HTCs in this study is protectedness. To our knowledge, this parameter has never been described in this setting. As stated before, protectedness is calculated automatically by the software and evaluates the length of not only the channel but also the protected part of it (part of the border zone protected by core tissue), which, mechanically, could be related to the preferential conduction of a VT isthmus. In our study, protectedness was the parameter most closely related to arrhythmogenicity in the univariate analysis and was the only parameter with statistical significance in the multivariate analysis. In summary, if an HTC is fully protected (high protectedness), it will have an increased probability of acting as part of a VT circuit; therefore, its arrhythmogenicity will be increased.

Potential scenarios for clinical application

The current substrate modification strategy for VT ablation targets an extensive substrate by identifying and ablating LPs and LAVAs to homogenize the entire scar. This strategy has been shown to reduce recurrent VT compared with other approaches,¹² although it is also related to long procedural times. In addition, the presence of LPs or LAVA is

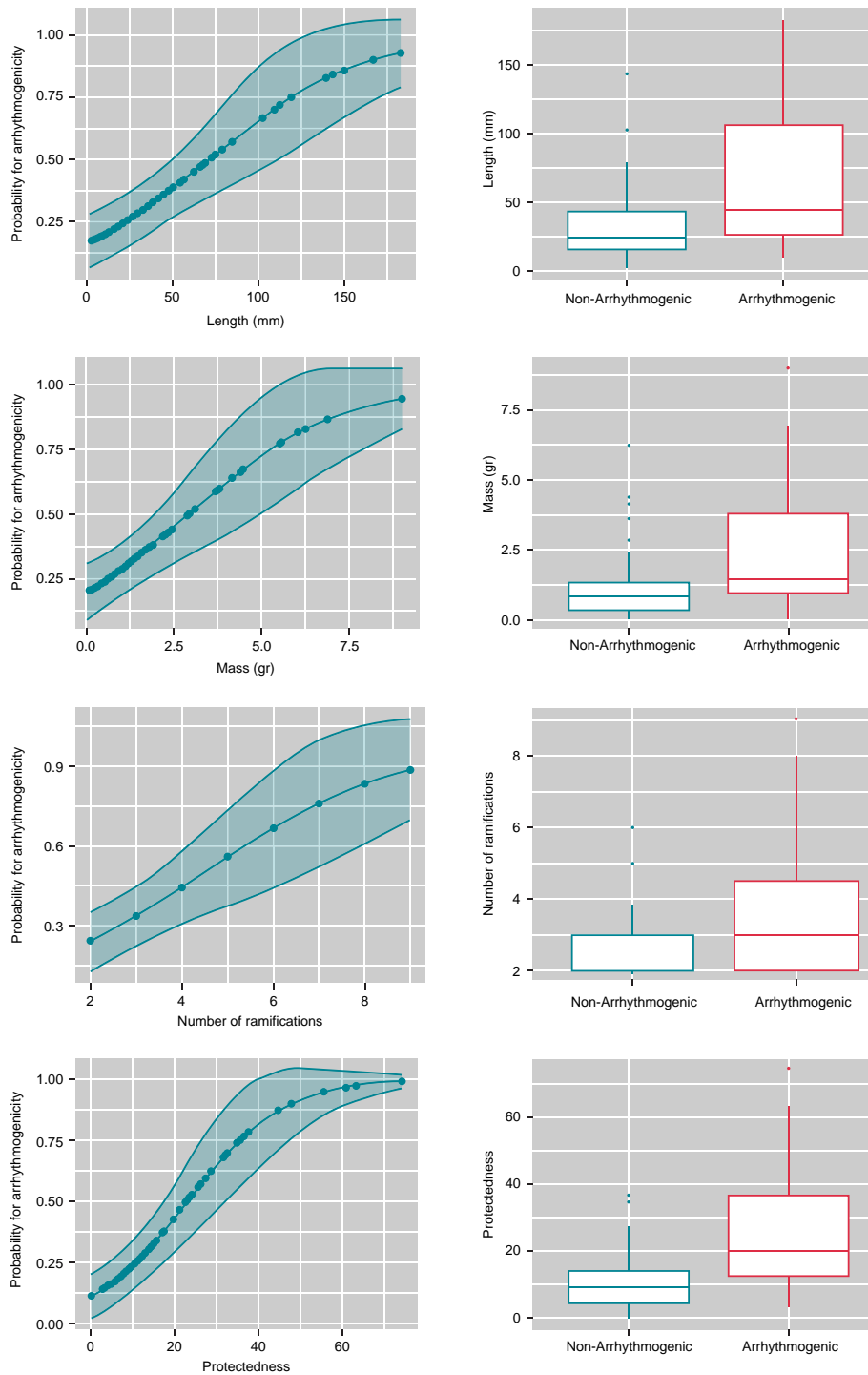


Figure 4 Predictions of the probability of arrhythmogenicity with logistic regression for length, mass, number of ramifications and protectedness.

not always involved in the VT circuits, and ablating the tissue that is not involved in the VT could create new areas of slow conduction that may predispose patients to new VT circuits.

To avoid the ablation of large areas of myocardium that are not linked to VT, different approaches have been proposed. Porta *et al.*¹³

demonstrated that decrement-evoked potential substrate mapping identified the functional substrate critical to the VT circuit with high specificity, suggesting that ablation could be limited to these areas without the need to target all LPs. On the other hand, Aziz *et al.*¹⁴ showed that DZs were highly arrhythmogenic, functioning as niduses for re-entry, and

Table 4 Multivariable analysis for the primary endpoints

Channel characteristic	Univariate OR (95% CI)	P-value	Multivariable OR (95% CI)	P-value
Length (mm)	1.02 (1.01–1.04)	<0.001		
Mass (grams)	1.62 (1.18–2.21)	<0.001		
Protectedness	1.09 (1.04–1.14)	<0.001	1.09 (1.04–1.14)	<0.001
Number of layers	1.31 (1.07–1.60)	0.008		
Number of ramifications	1.59 (1.15–2.19)	0.002		
Number of AHA segments	2.37 (1.4–4.04)	<0.001		

Mm, millimeter; AHA, American Heart Association; OR, odds ratio; CI, confidence interval. Bold values mean that there the values are statistically significant.

demonstrated the feasibility and effectiveness of VT ablation limited to the DZs identified by propagational analysis of ventricular activation during sinus rhythm, obviating the need for more extensive ablation.

Our work highlights the idea that arrhythmogenicity is limited to certain areas. In the same way that not all LPs seen on the EAM are involved in the VT circuits, not all the HTC identified by cardiac imaging are arrhythmogenic.

A meticulous examination of the substrate by LGE-CMR can help identify the arrhythmogenic HTCs responsible for a certain VT circuit. In combination with other strategies, the evaluation of the length, protectedness, number of ramifications or transmuralty of a given CC adds valuable information prior to a VT ablation procedure and helps in planning the best ablation strategy. More studies are needed to examine whether VT ablation procedures could be limited to the ablation of arrhythmogenic HTCs in the future, which could potentially reduce the procedural time and risks.

Overall, our findings allow us to better understand VT substrates with potential implications to plan VT ablation procedures. These results, if confirmed by other studies, add channel characteristics as new parameters to elucidate the arrhythmogenicity of scars for VT ablation. In addition, these parameters could also be used for patients with scarring and an left ventricular ejection fraction (LVEF) > 35% in whom guidelines do not recommend ICD implantation to improve arrhythmic risk stratification.

Limitations

This is a single centre study and one of the principal limitations is derived from the small sample size. Another limitation is the WB sequence acquisition (has a lower spatial resolution than 3 T conventional LGE-CMR).

Regarding ADAS software, some limitations need to be addressed. First, HTC detection by LGE-CMR in our manuscript is linked to this specific software, so the results may not be able to be extrapolated to other imaging software. Second, HTC identification was automatically performed by the software, but arrhythmogenic HTC identification was performed manually which makes it difficult to extrapolate the results to other centres with less experience in the interpretation of CMR. Furthermore, the CMR images and EAM were not merged and were analyzed side by side, which could create an error in spatial alignment.

Another limitation is the presence of epicardial HTCs on LGE-CMR in patients in whom only an endocardial approach was performed (therefore, they could have being incorrectly qualified as 'non-arrhythmogenic'). Although this is a limitation of our study, two points must be considered. First, only 16% of HTCs were purely epicardial or midmyocardial. In addition, if the patient was still inducible after endocardial ablation, a subxiphoid approach to map the epicardium was

performed, so arrhythmogenicity (considered to be inducible VT) was also mapped in the epicardium if needed.

Finally, after ablation of the induced VT, substrate ablation was performed, and only another induction test was performed after ablation. In this sense, some VTs could have been induced after ablation of the first VT in relation to other HTCs that, finally, could be misclassified as non-arrhythmogenic HTCs.

Conclusions

Scar channel characteristics such as length, mass, transmuralty and protectedness can be measured by LGE-CMR, may be related to the most likely re-entrant circuit and has a potential role in tailoring ablation strategies.

Acknowledgements

The authors want to thank Dr.Peng Hu (UCLA, Los Angeles, CA) for his pioneering work on wideband LGE. Also we want to thank Xiaoming Bi, PhD, and Siemens Healthineers for their support with the wideband sequence work in progress collaboration.

Funding

This work was supported in part by the Instituto de Salud Carlos III (ISCIII, grant n° PI20/00693), CIBERC16 (CB16/11/00354), the Agència de Gestió d'Ajuts Universitaris i de Recerca (AGAUR), the Recognized Research Group (2017-SGR-01548), and the CERCA Programme/Generalitat de Catalunya.

Conflict of interest: I.R.L. and J.M.T. have served as consultants for Boston Scientific and Abbott Medical.L.M. and J.B. report activities as consultants, lecturers, and advisory board members for Abbott Medical, Boston Scientific, Biosense Webster, Medtronic, and Biotronik. They are also shareholders of Galgo Medical, S.L. M.S and R.FV work for ADAS3D Medical S.L. All other authors declare no conflict of interest.

Data availability

The authors declare that the data that support the findings of this study are available from the corresponding author.

References

1. Wissner E, Stevenson WG, Kuck K-H. Catheter ablation of ventricular tachycardia in ischaemic and non-ischaemic cardiomyopathy: where are we today? A clinical review. *Eur Heart J* 2012;**33**:1440–50.
2. Stevenson WG, Khan H, Sager P, Saxon LA, Middlekauff HR, Natterson PD et al. Identification of reentry circuit sites during catheter mapping and radiofrequency ablation of ventricular tachycardia late after myocardial infarction. *Circulation* 1993;**88**(4): 1647–70.
3. Fitzgerald DM, Friday KJ, Wah JA, Lazzara R, Jackman WM. Electrogram patterns predicting successful catheter ablation of ventricular tachycardia. *Circulation* 1988;**77**(4): 806–14.

4. Andreu D, Berrueto A, Ortiz-Pérez JT, Silva E, Mont L, Borràs R et al. Integration of 3D electroanatomic maps and magnetic resonance scar characterization into the navigation system to guide ventricular tachycardia ablation. *Circulation: Arrhythmia and Electrophysiology* 2011;**4**(5):674–83.
5. Quinto L, Sánchez-Somonte P, Alarcón F, Garre P, Castillo À, San Antonio R et al. Ventricular tachycardia burden reduction after substrate ablation: predictors of recurrence. *Heart Rhythm* 2021;**18**(6):896–904.
6. Dickfeld T, Tian J, Ahmad G, Jimenez A, Turgeman A, Kuk R et al. MRI-Guided Ventricular tachycardia ablation. *Circulation: Arrhythmia and Electrophysiology* 2011;**4**(2):172–84.
7. Fernández-Armenta J, Berrueto A, Andreu D, Camara O, Silva E, Serra L et al. Three-Dimensional architecture of scar and conducting channels based on high resolution ce-CMR. *Circulation: Arrhythmia and Electrophysiology* 2013;**6**(3):528–37.
8. Andreu D, Penela D, Acosta J, Fernández-Armenta J, Perea RJ, Soto-Iglesias D et al. Cardiac magnetic resonance-aided scar dechanneling: influence on acute and long-term outcomes. *Heart Rhythm* 2017;**14**(8):1121–8.
9. Sánchez-Somonte P, Quinto L, Garre P, Zaraket F, Alarcón F, Borràs R et al. Scar channels in cardiac magnetic resonance to predict appropriate therapies in primary prevention. *Heart Rhythm* 2021;**18**(8):1336–43.
10. Roca-Luque I, van Breukelen A, Alarcon F, Garre P, Tolosana JM, Borràs R et al. Ventricular scar channel entrances identified by new wideband cardiac magnetic resonance sequence to guide ventricular tachycardia ablation in patients with cardiac defibrillators. *Europace* 2020;**22**(4):598–606.
11. Mahida S, Sacher F, Dubois R, Sermesant M, Bogun F, Haïssaguerre M et al. Cardiac imaging in patients with ventricular tachycardia. *Circulation* 2017;**136**(25):2491–2507.
12. di Biase L, Santangeli P, Burkhardt DJ, Bai R, Mohanty P, Carbucicchio C et al. Endo-Epicardial homogenization of the scar versus limited substrate ablation for the treatment of electrical storms in patients with ischemic cardiomyopathy. *J Am Coll Cardiol* 2012;**60**(2):132–41.
13. Porta-Sánchez A, Jackson N, Lukac P, Kristiansen SB, Nielsen JM, Gizurarson S et al. Multicenter study of ischemic ventricular tachycardia ablation with decrement-evoked potential (DEEP) mapping with extra stimulus. *JACC: Clinical Electrophysiology* 2018;**4**(3):307–15.
14. Aziz Z, Shatz D, Raiman M, Upadhyay GA, Beaser AD, Besser SA et al. Targeted ablation of ventricular tachycardia guided by wavefront discontinuities during Sinus rhythm. *Circulation* 2019;**140**(17):1383–97.